Since January 2020 Elsevier has created a COVID-19 resource centre with free information in English and Mandarin on the novel coronavirus COVID-19. The COVID-19 resource centre is hosted on Elsevier Connect, the company's public news and information website.

Journal of Pharmaceutical and Biomedical Analysis 217 (2022) 114827

Contents lists available at ScienceDirect

Journal of Pharmaceutical and Biomedical Analysis

journal homepage: www.journals.elsevier.com/journal-of-pharmaceutical-and-biomedical-analysis

Untargeted lipidomics reveals specific lipid profiles in COVID-19 patients with different severity from Campania region (Italy)

Michele Ciccarelli [a,1], Fabrizio Merciai [c,d,1], Albino Carrizzo [a,b], Eduardo Sommella [c], Paola Di Pietro [a], Vicky Caponigro [c], Emanuela Salviati [c], Simona Musella [c], Veronica di Sarno [c], Mariarosaria Rusciano [a], Anna Laura Toni [a], Paola Iesu [a], Carmine Izzo [a], Gabriella Schettino [e], Valeria Conti [a], Eleonora Venturini [b], Carolina Vitale [e], Giuliana Scarpati [e], Domenico Bonadies [e], Antonella Rispoli [e], Benedetto Polverino [e], Sergio Poto [e], Pasquale Pagliano [a], Ornella Piazza [a], Danilo Licastro [f], Carmine Vecchione [a,b,*,1,2], Pietro Campiglia [c,**,1,2]

[a] Department of Medicine and Surgery, University of Salerno, Baronissi, SA, Italy
[b] IRCCS Neuromed, Loc. Camerelle, Pozzilli, IS, Italy
[c] Department of Pharmacy, University of Salerno, Fisciano, SA, Italy
[d] PhD Program in Drug Discovery and Development, University of Salerno, Fisciano, SA, Italy
[e] San Giovanni di Dio e Ruggi D'Aragona University Hospital, Salerno, Italy
[f] AREA Science Park Padriciano, 9934149 Trieste, Italy

ARTICLE INFO

Keywords:
COVID-19
Lipidomics
Severity
Trapped ion mobility
Untargeted

ABSTRACT

COVID-19 infection evokes various systemic alterations that push patients not only towards severe acute respiratory syndrome but causes an important metabolic dysregulation with following multi-organ alteration and potentially poor outcome. To discover novel potential biomarkers able to predict disease's severity and patient's outcome, in this study we applied untargeted lipidomics, by a reversed phase ultra-high performance liquid chromatography-trapped ion mobility mass spectrometry platform (RP-UHPLC-TIMS-MS), on blood samples collected at hospital admission in an Italian cohort of COVID-19 patients (45 mild, 54 severe, 21 controls). In a subset of patients, we also collected a second blood sample in correspondence of clinical phenotype modification (longitudinal population). Plasma lipid profiles revealed several lipids significantly modified in COVID-19 patients with respect to controls and able to discern between mild and severe clinical phenotype. Severe patients were characterized by a progressive decrease in the levels of LPCs, LPC-Os, PC-Os, and, on the contrary, an increase in overall TGs, PEs, and Ceramides. A machine learning model was built by using both the entire dataset and with a restricted lipid panel dataset, delivering comparable results in predicting severity (AUC= 0.777, CI: 0.639–0.904) and outcome (AUC= 0.789, CI: 0.658–0.910). Finally, re-building the model with 25 longitudinal (t1) samples, this resulted in 21 patients correctly classified. In conclusion, this study highlights specific lipid profiles that could be used monitor the possible trajectory of COVID-19 patients at hospital admission, which could be used in targeted approaches.

Abbreviations: RT, retention time; CCS, Collision Cross Section; CEs, cholesteryl esters; DGs, diacylglycerols; TGs, triacylglycerols; LPCs, lysophosphatidylcholines; LPC-Os, ether-linked lysophosphatidylcholines; PCs, phosphatidylcholines; PC-Os, ether-linked phosphatidylcholine; PEs, phosphatidylethanolamines; Cer, Ceramides; TIMS-MS, Trapped ion mobilty mass spectrometry.

* Corresponding author at: Department of Medicine and Surgery, University of Salerno, Baronissi, SA, Italy.
** Corresponding author.
E-mail addresses: cvecchione@unisa.it (C. Vecchione), pcampiglia@unisa.it (P. Campiglia).
[1] These authors share first authorship
[2] These authors share last authorship

https://doi.org/10.1016/j.jpba.2022.114827
Received 21 February 2022; Received in revised form 4 May 2022; Accepted 5 May 2022
Available online 10 May 2022

1. Introduction

The current pandemic caused by severe acute respiratory syndrome coronavirus 2 (SARS-CoV-2) is still delivering an enormous impact on health management globally. Indeed, the scarce vaccination practice in countries with weaker health and economic systems makes COVID-19 still a relevant health and social problem worldwide [1]. While roughly 80% of COVID-19 patients show only mild symptoms, conditions can rapidly evolve to severe phenotype. The pathophysiology of COVID-19 is indeed highly complex; beyond immune changes, metabolism emerged as a critical regulator that is tightly bound to the host response and involved in the disease's progression [2]. Some patients with COVID-19 undergo an altered metabolic state, known as "phenoconversion" [3], predictive of multi-organ alteration and poor outcome. Specifically, clinical deterioration in patients with COVID-19 involves multiple pathways, including chemotaxis and interleukin production, but also endothelial dysfunction, the complement system, and immunothrombosis. Indeed, unfavorable outcome in hospitalized COVID-19 patients has been previously associated with changes in concentrations of IL-6, IL-8, IL-10, soluble Receptor for Advanced Glycation End Products (sRAGE), vascular cell adhesion molecule 1 (VCAM-1) and Pentraxin-3 [4]. Moreover, also lipids play various critical biological functions in cellular barriers, signal transduction, material transport, energy storage, cell differentiation, and apoptosis. SARS-CoV-2 can induce characteristic molecular changes detected in patients' sera using proteomic and metabolomic technologies [5,6] which also correlates with modification of the inflammatory profile of the COVID-19 patients [7]. Therefore, omic sciences, such as metabolomics and lipidomics, can be instrumental in identifying predictive biomarkers of severity and progression, monitoring the metabolic status of individuals during the time and thus applied to evaluate the metabolic host response to SARS-CoV-2 infection. In this regard, lipids cover a crucial role in numerous metabolic processes, such as energy management and storage, act as structure and membrane components, and are essential players in cell signaling. They have also been found deeply dysregulated in other viral infections, like Ebola virus disease (EVD) [5,8–10]. Lipids are essential also in the life cycle of SARS-CoV-2, which is an envelope virus surrounded by a lipid bilayer, furthermore, following infection, host immune cells like macrophages show a change in lipid metabolism upon activation, which is tightly connected to the immune response to pathogens [11]. Initial studies have in fact evidenced that eicosanoids dysregulation, as well as lower serum HDL levels are connected with disease severity and mortality rate [12, 13]. Therefore lipidomics, with its potential to identify and quantify several lipid subclasses in a single analysis [14], can be a useful tool for a better comprehension of COVID-19 physiopathology and identification of novel therapeutic strategies. In this regard, targeted [7, 15] and untargeted mass spectrometry-based lipidomics studies [6, 16] have been carried out on different COVID-19 cohorts. All these studies, even if heterogeneous and carried out with different technologies, evidenced a profound dysregulation in plasma lipidome of COVID-19 patients, such as increased sphingomyelins (SM) and reduced diacylglycerol (DG) levels [10], increased ceramides (Cer) and triglycerides (TG) [9], and generally decreasing glycerophospholipids [6] even with conflicting results [9, 10]. Overall, lipid biomarkers mirror the severity statuses, but their effective predictive potential has not been clearly identified. Thus, we hypothesize that metabolic changes in COVID-19 patients are earlier than clinical changes and, therefore, potentially exploitable for early prognostic assessment. In this study, to uncover the lipid changes in the plasma of COVID-19 patients, we applied an untargeted lipidomics approach, by ultra-high-performance liquid chromatography coupled trapped ion mobility mass spectrometry (UHPLC-TIMS-MS), in an Italian cohort of hospitalized COVID-19 patients. We highlight a profound alteration of different lipid subclasses, particularly a significant and progressive decrease of glycerophospholipids, already at the time of admission, and explored the potential capability of a specific lipid subset to predict COVID-19 patients' outcome.

2. Material and methods

2.1. Study design and participants

A cohort of 99 patients with a positive nasopharyngeal/oropharyngeal swab PCR test for COVID-19 (SARS-CoV-2 infection) was enrolled between October 2020 and March 2021 at the University Hospital "Giovanni Da Procida", Salerno, Italy. None of these patients were vaccinated against COVID-19. The cohort's median age was 68 years old, and the female proportion was 61%. At admission, patients were classified according to the clinical phenotype following World Health Organization (WHO) severity score as *Mild* patients (hospitalized patients requiring or not supplemental oxygen; n = 45), or *Severe* patients (hospitalized patients requiring non-invasive ventilation or high-flow oxygen therapy; intubation and mechanical ventilation, or ventilation with additional organ support; n = 54) [World Health Organization. WHO R&D Blueprint. Novel Coronavirus: COVID-19 Therapeutic Trial Synopsis. Draft February 18, 2020.www.who.int/blueprint/priority-diseases/key-action/COVID-19_Treatment_Trial_Design_Master_Protocol_synopsis_Final_18022020.pdf]. Patients were further followed up until hospital discharge or death and subdivided into survivors (Mild, n = 37; Severe, n = 20) and non-survivors (Mild, n = 8; Severe, n = 34). Blood samples from all patients were collected at the time of admission (Time 0). In a subgroup of patients (n = 25) we collected a second blood sample (Time 1) in correspondence of clinical and symptoms changes (phenotypical switch).

Healthy and SARS-CoV-2 negative subjects (n = 21) of age 50.21 ± 10.29% and 50% of females were recruited from healthcare workers at the University Hospital "San Giovanni di Dio e Ruggi d'Aragona". The study protocol was approved by the local Ethics Committee (prot./SCCE no. 71262, May 2020). All methods and experimental procedures were performed under the Declaration of Helsinki.

2.2. Blood sample processing

Blood samples were collected in fasting states. From each patient, 5–8 mL of whole blood was drawn into EDTA vacutainers and centrifuged at 1000 × *g* for 20 min at 25 °C to separate blood cells and plasma. After collection, plasma samples were aliquoted and stored at – 80 °C until analysis.

2.3. Plasma lipidome extraction

Before extraction, samples were randomized and split in regular subgroups. Lipids were extracted following the Matyash et al. protocol [17], with slight modifications: briefly, 20 μL of plasma were thawed on ice and added to 225 μL of ice cold MeOH containing a mix of deuterated standards (Splash Lipidomix®, Avanti Polar Lipids, Alabaster, AL, U.S.A) and vortexed for 10 s. Subsequently, 750 μL of cold methyl tert-butyl ether (MTBE) were transferred to the tube and the solution was shaken in a thermomixer (Eppendorf) for 10 min, 300 rpm at 4 °C. Then, 188 μL of H_2O were added and samples were vortexed for 20 s and centrifuged at 14,680 rpm, for 10 min at 4 °C to induce phase separation. The upper layer was collected and evaporated using a SpeedVac (Savant, Thermo Scientific, Milan, Italy). The dried samples were dissolved in 100 μL of BuOH/IPA/H_2O 8/23/69 (*v/v*) before the UHPLC-TIMS analysis. A quality control (QC) sample was prepared by pooling the same aliquot (3 μL) from each sample. Unless otherwise described, all solvents and additives were LC-MS grade and purchased by Merck (Darmstadt, Germany).

2.4. RP-UHPLC-TIMS-MS method parameters

UHPLC-TIMS analyses were performed on a Thermo Ultimate RS

3000 UHPLC coupled online to a TimsTOF *Pro* quadrupole Time of flight (Q-TOF) (Bruker Daltonics, Bremen, Germany) equipped with an Apollo II electrospray ionization (ESI) probe. The separation was performed with an Acquity UPLC CSH C18 column (100 × 2.1 mm; 1.7 μm) protected with a VanGuard CSH precolumn (5.0 × 2.1 mm; 1.7 μm, 130 Å) (Waters, Milford, MA, U.S.A). The column temperature was set at 55 °C, a flow rate of 0.4 mL/min was used, mobile phase consisted of (A): ACN/H_2O with 10 mM $HCOONH_4$ and 0.1% HCOOH 60:40 (*v/v*) and (B): IPA/ACN with 10 mM HCOONH4 and 0.1% HCOOH 90:10 (*v/v*). The following gradient has been used: 0 min, 40% B; 2 min, 43% B; 2.10 min, 50% B; 12 min, 54% B; 12.10 min, 70% B; 17 min, 99% B; 17.10 min, 99% B; 17.2, 40% B and then 2.8 min for column re-equilibration. The analyses were performed in data-dependent parallel accumulation serial fragmentation (DDA-PASEF) with both positive and negative ionization, in separate runs. The injection volume was set at 3 μL for the positive mode and 5 μL for the negative mode. Source parameters: Nebulizer gas (N_2) pressure: 4.0 Bar, Dry gas (N_2): 10 l/min, Dry temperature: 250 °C. Mass spectra were recorded in the range *m/z* 100–1500, with an accumulation and ramp time to 100 ms each. The ion mobility was scanned from 0.55 to 1.70 Vs/cm^2. Precursors for data-dependent acquisition were isolated within ± 2 *m/z* and fragmented with an ion mobility-dependent collision energy, 30 eV in positive mode, and 40 eV in negative mode. The total acquisition cycle was of 0.32 s and comprised one full TIMS-MS scan and two PASEF MS/MS scans. Exclusion time was set to 0.1 min, Ion charge control (ICC) was set to 7.5 Mio. The instrument was calibrated for both mass and mobility using the ESI-L Low Concentration Tuning Mix with the following composition: [*m/z*, $1/K_0$: (322.0481, 0.7318 Vs cm^{-2}), (622.0290, 0.9848 Vs cm^{-2}), (922.0098, 1.1895 Vs cm^{-2}), (1221,9906, 1.3820 Vs cm^{-2})] in positive mode and [*m/z*, $1/K_0$: (301.99814, 0.6678 Vs cm^{-2}), (601.97897, 0.8781 Vs cm^{-2}), (1033.98811, 1.2525 Vs cm^{-2}), (1333.96894, 1.4015 Vs cm^{-2})] in negative mode.

2.5. RP-UHPLC-TIMS-MS data analysis and processing

4D data alignment, filtering and annotation was performed with MetaboScape 2021 (Bruker) employing a feature finding algorithm (T-Rex 4D) that automatically extracts buckets from raw files. At the beginning of each LC-MS run, a mixture (1:1 *v/v*) of 10 mM sodium formate calibrant solution and ESI-L Low Concentration Tuning Mix was injected to recalibrate, respectively, both the mass and mobility data. Feature detection was set to 500 and 250 counts for positive and negative modes. The minimum number of data points in the 4D TIMS space was set to 100, and recursive feature extraction was used (75 points). Lipid annotation was performed first with a Rule-based annotation and, subsequently, using the LipidBlast spectral library of MS DIAL (http://prime.psc.riken.jp/compms/msdial/main.html) with the following parameters: tolerance: narrow: 2 ppm, wide: 10 ppm; mSigma: narrow 30, wide 250, MS/MS score: narrow 800, wide 150. Collision Cross Section (CCS)%: narrow 2, wide 5. The spectra were processed using $[M+H]^+$, $[M+Na]^+$, $[M+K]^+$, $[M+H\text{-}H_2O]^+$ and $[M+NH_4]^+$ ions in positive mode, while $[M–H]^-$, $[M+Cl]^-$, $[M+HCOO]^-$ and $[M\text{-}H_2O]^-$ in negative mode. CCS values were further compared with the those predicted by LipidCSS tool (http://www.metabolomics-shanghai.org/LipidCCS/), the assignment of the molecular formula was performed for the detected features using Smart Formula™ (SF). For the assessment of repeatability and instrument stability over time, a QC strategy was applied [18] using pooled plasma samples inserted during the batch regularly together with a mixture of authentic lipid standards [LightSPLASH®, Avanti Polar Lipids] to monitor specific retention time and response modification of lipid subclasses. Samples were injected in randomized order and blank samples (blank matrix extracted, e.g following all the steps of extractions, and neat solvent used for sample solubilization) were injected regularly and used to assess and exclude background signals.

2.6. Statistical analysis

Univariate and multivariate statistics was performed with MetaboAnalyst 5.0 (https://www.metaboanalyst.ca). Data preprocessing consisted of the following steps: all lipids missing in more than 50% in QCs and 75% in real samples were excluded, furthermore all lipids with a coefficient of variation (CV%) higher than 35% among QCs samples were discarded. In order to flatten the differences between samples and to avoid bias in the statistical analysis, we first normalized lipid intensities with the corresponding deuterated internal standard [19] and then the dataset was log transformed and auto scaled. A preliminary investigation was carried out using Principal Component Analysis (PCA) on pre-processed data. Then, Partial Least Square Discriminant Analysis (PLS-DA) model was built in order to discriminate between healthy patients and mild and severe covid patients. K-fold cross-validation was performed, splitting the data into 10 subgroups to select the optimal number of Latent Variables (nLVs). The nLVs were selected maximizing the accuracy in cross validation. PLS-DA solves classification problems with more than 2 classes and in the scenario where there is a high number of variables and low samples. Statistical analysis between patients' characteristics were analyzed using student *t* test using SPSS v25. Variable importance in projection (VIP) scores, based on PLS-DA results, and Significance analysis of Metabolomics (SAM), giving a delta value of 1.5, were used to identify lipids responsible for the maximum separation of the groups. For univariate data analysis, one-way ANOVA corrected by Fisher's LSD post hoc analysis for intergroup comparison (Covid (-), Mild, Severe) was performed, setting a threshold of significance of false discovery rate (FDR) adjusted *p*-value of 0.01. Volcano plot analysis was used to visualize significant lipids between Mild and Severe patients (Folch-change: 1.5, pvalue: 0.05 FDR). Receiver operating characteristic (ROC) analysis was carried out with the Biomarker analysis tool in Metaboanalyst 5.0. A random forest (RF) machine learning (ML) algorithm was performed, after splitting the cohort in a training set and a test set, was tested as a predictive model. Lipid features were ranked according to the specific metrics of each modeling method (*p*-values, absolute loading values from PCA, the variable importance in projection from PLS-DA, delta value on SAM analysis, and the feature importance from the RF model). A multivariate ROC curve model was compared with the whole lipid profile.

3. Results and discussion

3.1. Untargeted lipidomics analysis of COVID-19 plasma samples

Untargeted lipidomics analyses were conducted with an RP-UHPLC-TIMS-MS strategy summarized in Fig. 1. System repeatability was assessed by a pooled QC strategy, which closely clustered as can be observed from PCA score plot (Fig. S1), while lipid annotations were performed following the lipidomic standard initiative guidelines (Fig. S2). (https://lipidomics-standards-initiative.org/). In detail our initial workflow started from 994 annotations which were subjected to several filters: mass accuracy (Δppm: max 5.0 ppm), collision section error values (ΔCCS: max 5%), peak shape, most probable adduct form, MS/MS spectral similarity score, RT and CCS values linearity, carryover, and CV < 35% in QCs. As a result, retention time reproducibility resulted in a median CV value of 0.42%, prior to the RT alignment, while average MS/MS score, Δppm and ΔCCS were respectively: 914.60 MS/MS score, 0.60 Δppm, 1.30% ΔCCS (Fig. S2). After further manual curation, 348 unique lipids belonging to 16 subclasses (Fig. S3) were annotated with high confidence (table S1), in this regard, for more than 75% of lipids CV values were < 20%, and for the remaining 25%, CV was < 30%. Notably, 91.67% of the annotations were in common between rule based and spectral library approaches, moreover the implementation of trapped ion mobility ensured further confidence in lipid annotation, by comparison of experimental CCS values with those reported in libraries. Following raw data alignment, filtering and annotation as

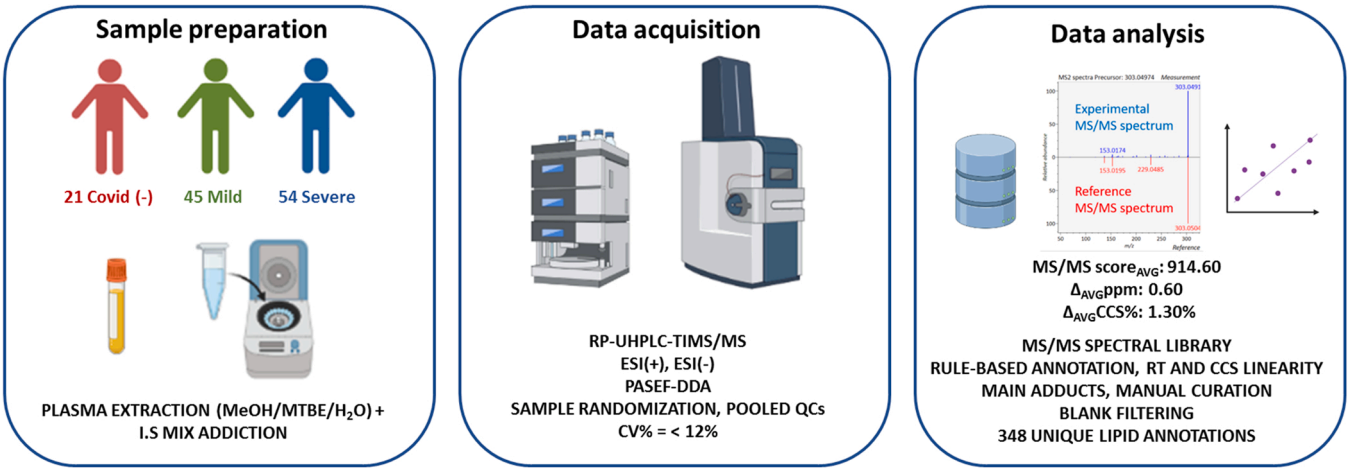

Fig. 1. Workflow of the untargeted lipidomics approach: 120 plasma samples were extracted and analyzed by RP-UHPLC-TIMS/MS, repeatability was assessed by a pooled QC strategy, lipid annotation was performed by spectral library comparison, rule-based annotation, retention time and Collision Cross Section linearity.

described in Section 2.5, for each lipid feature the precursor ion response was normalized against the class-specific internal standard, as widely reported for untargeted lipidomics approaches [18]. Results were expressed as nmol/mL and reported in Supplementary table S4.

3.2. Clinical features of COVID-19 patients

In our cohort, no significant differences in baseline characteristics were identified at admission between mild and severe patients. We found a slight prevalence of female patients with no difference of age between mild and severe phenotype. For all the comorbidities analyzed we did not detect a significant difference between the two groups. Furthermore, we subdivided mild and severe groups into "survivors" and "non-survivors" considering death as final endpoint. The demographic and comorbidities information are summarized in Table 1. In the mild group no demographic and prevalence comorbidities differences were found between "survivors'' and "non-survivors" except for valvular disease and peripheral arterial disease (PAD), (1 patient in "non-survivor" group). The same observation was for the severe group except for the presence of PAD (1 patient in the "survivor" group). Data are reported in Tables 2 and 3.

Table 1
Clinical characteristics of COVID-19 patients subdivided by phenotype at admission; CAD: coronary artery diseases; HF: heart failure; PAD: peripheral artery disease; CKD: chronic kidney disease; COPD: Chronic obstructive pulmonary disease.

	Covid (+)		
	Mild (45)	Severe (54)	*p*-value
Sex	F: 23 (51.1%); M: 22 (48.9%)	F: 38 (70.4%); M: 16 (29.6%)	0.05
Age	67.91 ± 17.22	67.85 ± 11.62	0.984
CAD	7 (15.6%)	12 (22.2%)	0.475
HF	4 (8.9%)	2 (3.7%)	0.068
Obesity	4 (8.9%)	12 (22.2%)	0.905
Atrial Fibrillation	6 (13.3%)	5 (9.3%)	0.124
Valvular disease	1 (2.2%)	2 (3.7%)	0.863
PAD	1 (2.2%)	1 (1.9%)	0.490
Dyslipidemia	6 (13.3%)	8 (14.8%)	0.280
Diabetes mellitus	14 (31.1%)	17 (31.5%)	0.119
Arterial hypertension	26 (57.8%)	32 (59.3%)	0.093
CKD	7 (15.6%)	7 (13.0%)	0.513
Smoking	3 (6.7%)	7 (13.0%)	0.597
COPD	10 (22.2%)	9 (13.7%)	0.062
Autoimmune Disease	1 (2.2%)	4 (7.4%)	0.738

3.3. Differential lipidomic signature discerns between COVID-19 phenotypes

For lipidomic analysis, exploratory analysis was performed by unsupervised principal component analysis (PCA) which showed that the first 24 components explained the 95% of total variance (Fig. S1). To visualize classes separation supervised partial least square discriminant analysis (PLS-DA) was used. As shown in Fig. 2A and B PLS-DA score plots clearly differentiated the healthy controls COVID-19(−) from COVID-19 (+) patients, while in the context of COVID-19 group, the PLS-DA score could still discriminate between mild and severe phenotypes. The lipid features that contributed to the class separation and discrimination between the three groups were reported according to their variable of importance in projection (VIP) scores, extracted by PLS-DA. The 15 highest scoring VIP lipids (VIP score ≥ 1.8) are shown in Fig. 2C. Interestingly 9/15 lipids were lysophosphatidylcholines, in particular: six LPCs (LPC 20:1, LPC 18:0, LPC 20:2, LPC 17:0, LPC 16:0, LPC 18:1) three ether-linked LPCs (LPC O-16:0, LPC O-18:1, LPC O-16:1), two ether-linked phosphatidylcholines (PC O-34:3, isomers),

Table 2
Subdivision of COVID-19 Mild patients by outcome in "survivors" and "non-survivors"; CAD: coronary artery diseases; HF: heart failure; PAD: peripheral artery disease; CKD: chronic kidney disease; COPD: Chronic obstructive pulmonary disease.

	Mild "survivors" (37)	Mild "non-survivors" (8)	*p*-value
Sex	F: 19 (51%); M: 18 (49%)	F: 3 (37.5%); M: 5 (62.5%)	0.489
Age	65.24 ± 17.33	80.25 ± 10.37	0.024
CAD	5 (13.5%)	2 (25.0%)	0.307
HF	3 (8.1%)	1 (12.5%)	0.637
Obesity	4 (10.8%)	–	0.317
Atrial Fibrillation	4 (10.8%)	2 (25.0%)	0.355
Valvular disease	–	1 (12.5%)	0.040
PAD	–	1 (12.5%)	0.008
Dyslipidemia	4 (10.8%)	2 (25.0%)	0.201
Diabetes mellitus	12 (32.4%)	2 (25.0%)	0.835
Arterial hypertension	22 (59.5%)	4 (50.0%)	0.364
CKD	4 (10.8%)	3 (37.5%)	0.195
Smoking	1 (2.7%)	2 (25.0%)	0.006
COPD	6 (16.2%)	4 (50.0%)	0.014
Autoimmune disease	1 (2.7%)	2 (25.0%)	0.700

Table 3
Subdivision of COVID-19 Severe patients by outcome in "survivors" and "non-survivors"; CAD: coronary artery diseases; HF: heart failure; PAD: peripheral artery disease; CKD: chronic kidney disease; COPD: Chronic obstructive pulmonary disease.

	Severe "survivors" (20)	Severe "non-survivors" (34)	*p*-value
Sex	F: 6 (30%); M: 14 (70%)	F: 10 (29%); M: 24 (71%)	0.964
Age	65.00 ± 14.40	69.53 ± 9.47	0.169
CAD	5 (25.0%)	7 (20.6%)	0.673
HF	1 (5.0%)	1 (2.9%)	0.684
Obesity	6 (30.0%)	6 (17.6%)	0.196
Atrial Fibrillation	1 (5.0%)	4 (11.8%)	0.416
Valvular disease	1 (5.0%)	1 (2.9%)	0.662
PAD	1 (5.0%)	–	0.187
Dyslipidemia	5 (25.0%)	3 (8.8%)	0.108
Diabetes mellitus	4 (20.0%)	13 (38.2%)	0.277
Arterial hypertension	12 (60.0%)	20 (58.8%)	1.000
CKD	3 (15.0%)	4 (11.8%)	0.480
Smoking	6 (30.0%)	1 (2.9%)	0.090
COPD	3 (15.0%)	6 (17.6%)	0.776
Autoimmune disease	1 (5.0%)	3 (8.8%)	0.642

whose levels were all lower in COVID-19 patients. The remaining four lipids were TGs (TG 18:1_18:2_22:6, TG 18:1_18:1_22:6, TG 16:0_18:1_22:5, TG 16:0_20:4_22:6) which, inversely, display upregulation in COVID-19 patients. We next performed univariate comparison on the internal standard normalized, log transformed and auto scaled dataset. A total of 191 out of 348 lipids were found significantly modulated ($p < 0.01$, FDR: 0.01%, complete results are reported in Table S2) across the different classes. Noteworthy, ANOVA and significance analysis of metabolomics (SAM, Table S3) shared six metabolites which were top listed as significant in all compared conditions namely: LPC 20:1; LPC O-16:0, LPC O-18:1, LPC 18:0, PC O-34:3 and LPC O-16:1. These features were also listed among the significant lipids whose concentration was decreased in severe condition, as highlighted in the top left corner of the volcano plot in Fig. 2D. The heatmap, based on the top 30 lipid features (Fig. 2E, *p*-value < 0.01), evidences the lipidome signature that characterizes two different severity status. In particular, severe group is mostly associated to decrease of LPCs, LPC-Os, and PC-O. Contrariwise, severe status is characterized by an increase in TGs (TG 18:0_18:2_18:5; TG 18:1_18:2_18:2) and PEs (PE 34:1; PE 16:0_18:1; PE 18:1_18:0; PE 18:0_18:1) levels.

3.4. Lipidome signature predicts COVID-19 severity and outcome

The different lipid patterns between the control and COVID-19 group, and in particular, their progression along the phenotypes (from mild to severe), suggests that the lipidome signature measured at hospital admission could reflect the progression of disease and outcome. Therefore, to unveil the predictive potential of the discovered lipidome signature, we built a Random Forest (RF) machine learning (ML) model. The entire dataset was randomly divided into a training set, which was used to optimize and train the model, and a test set, to evaluate the model performance, which was assessed by area under curve (AUC) values of Receiver Operating Characteristic (ROC) curve. The model was trained on the complete annotated lipidome dataset (348 lipid features), by using repeated random subsampling cross validation (repeats = 100), the significance of the model's fit was computed using a permutation test with n = 1000 obtaining a p-value of 0.005. The model reached AUC values of 0.751 (95% CI: 0.599–0.887) for severity and 0.815 (95% CI: 0.662–0.944) for outcome respectively; the ROC curves are reported in Fig. 3A and B. The measurement of a large number of metabolites is challenging for potential fast clinical applications, which on the other hand would be easier with a reduced panel of the highest predictive

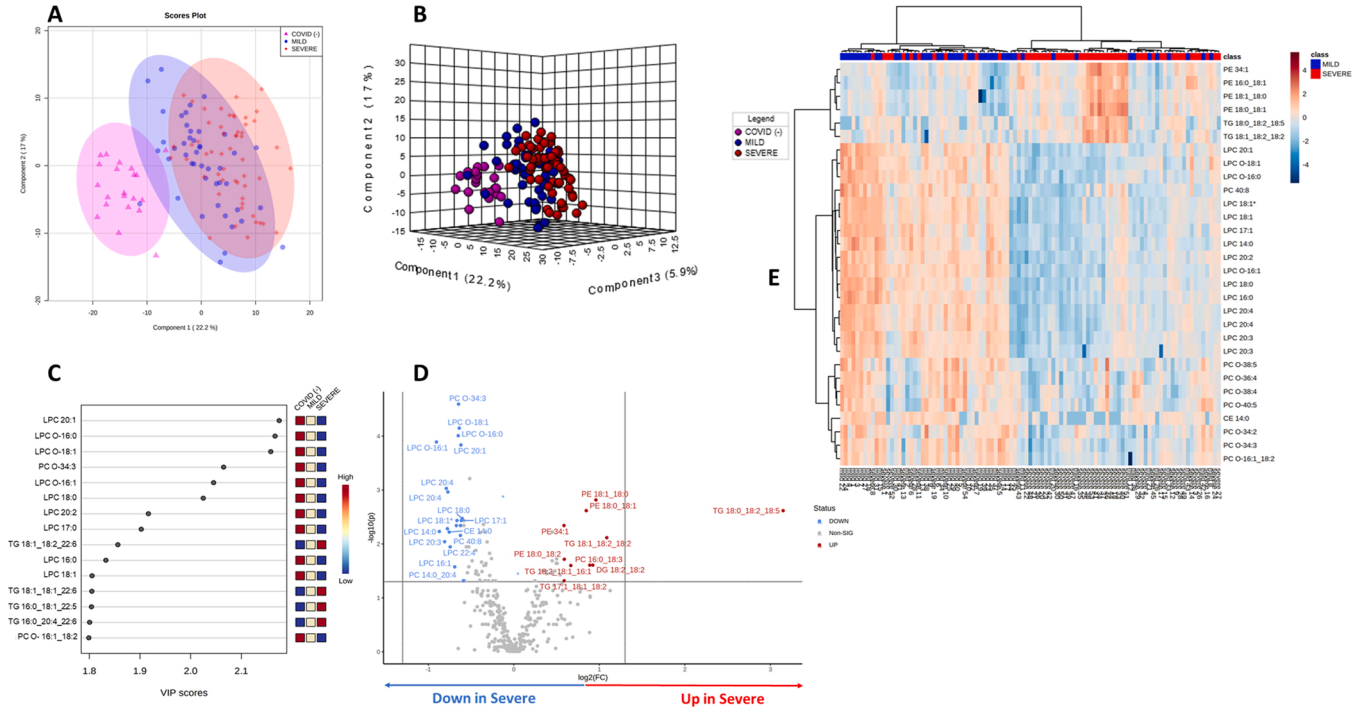

Fig. 2. A-E: 2D (A) and 3D (B) PLS-DA model score plot showing the discrimination of different classes: Covid (−): pink, mild: blue, severe: red; (C) The 15 highest scoring variables importance in projection (VIP) lipids are shown. The number of VIPs was established by setting the VIP-score ≥ 1.8 as a cutoff value. The colored boxes on the right indicate the relative amount of the corresponding lipid compound in each group; (D) Volcano plot graph illustrating unsignificant (gray) and significant compounds (blue: down-regulated, red: up-regulated) between Mild and Severe patients. The X-axis represent the log2FC (fold-change) and the Y-axis the -log10p (pvalue); (E) Heatmap reporting the top 30 lipid compounds based on the univariate statistical analysis (ANOVA, *p*-value < 0.001, FDR < 0.01%), the colors reflect the normalized lipid concentration in Mild (blue) and Severe (red) patients.

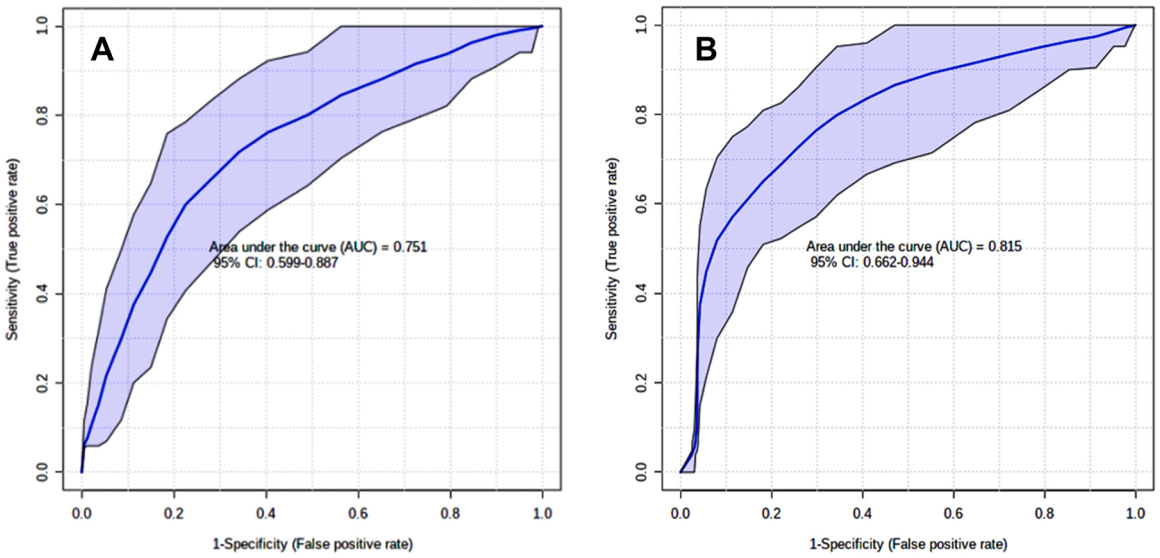

Fig. 3. A, B: ROC curves for severity (A) and outcome (B) obtained with the predictive model (RF) on the complete lipidome signature.

compounds. Therefore, we aimed to evaluate which lipids could accurately discriminate mild from severe conditions, among the 90 unique lipids that contributed to the model. Hence after a rank aggregation based on the previous models, a final panel of six lipids was built, and their ROC curves are reported in Fig. 4. The panel was composed by: LPC O-18:1 (AUC: 0.858, SE: 80%, SP: 81%), LPC O-16:1 (AUC: 0.855, SE: 86%, SP: 75%), LPC O-16:0 (AUC: 0.865, SE: 75%, SP: 90%), PC O-34:3 (AUC: 0.846, SE 80%, SP: 80%), LPC 20:1 (AUC: 0.815, SE: 7815, SP:75%), LPC 18:0 (AUC: 0.800, SE: 65%, SP: 75%), p-value < 0.001. By using this restricted panel of lipids, the RF results highlighted a comparable predictive potential, with similar AUC values to the model built on the complete lipid profile, for severity (AUC= 0.777, 95% CI:

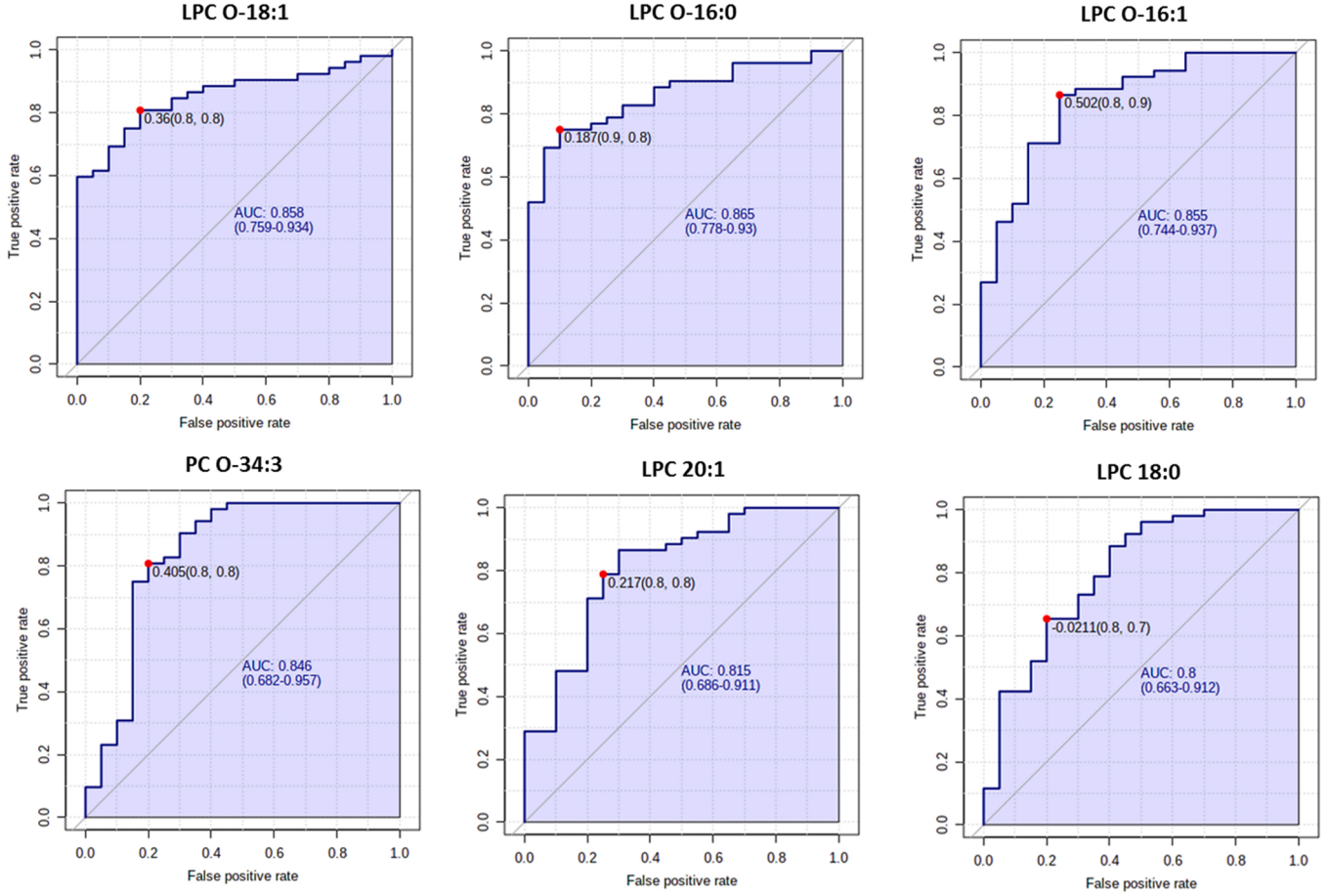

Fig. 4. ROC curves with the optimal cutoff calculated for each ROC analysis of the restricted lipid panel composed by LPC O-18:1, LPC O-16:1, LPC O-16:0, PC O-34:3, LPC 20:1, LPC 18:0.

0.639–0.904, Fig. 5) and outcome (AUC= 0.789, 95% CI: 0.658–0.910, Fig. 6) respectively. These results are in line to other studies in which metabolomics have been used to identify metabolites associated to the severity status [20, 21]. The model performance in cross validation for both analyses are comparable. In terms of accuracy and Monte Carlo Cross validation (MCC), severity and outcome RF models achieved both 75% and ~0.50. Sensitivity and specificity are 73% and 78% for the mild class while for the survivor class are 69% and 81% respectively. Applying the model to the external test set the severity is predicted with accuracy of 70% and 0.41 MCC. The sensitivity of mild class prediction is 88% and specificity is 50%. While for the outcome model, the test set is predicted with accuracy of 67% and MCC of 0.32; sensitivity and specificity were 71% and 62% respectively for the survivor class. Accordingly, LPCs, LPC-Os and PC-O levels were significantly lower in the severe group with respect to mild (Fig. 5). The evaluation of the same lipids' panel in the subdivision of patients into survivors and non-survivors revealed the predictive potential of these molecules, which appeared substantially reduced in the non-survivor group (Fig. 6) as compared both to healthy subjects and survivors. Moreover, the LPCs, LPC-Os and PC-O levels in survivor and non-survivor have been evaluated for each phenotype (mild and severe). Again, in the severe group, their levels were consistently lower in non-survivor as compared to survivors (Fig. S5). The identified lipid panel could be used not only at t0 but over the course of the disease. In fact, re-building the model with the 25 longitudinal (t1) patients, 21 were correctly classified for their outcome, survivors and non survivors, showing the ability of the lipid panel in highlighting the dynamic changes of disease (Fig. 7). Several conditions and demographic factors, such as age and comorbidities, predispose to a severe COVID-19 phenotype or even fatal outcome [22]. As indicated in Tables 1–3, sex and age represent the only demographic factors within our patient cohort that resulted statistically significant between mild and severe groups. Thus, we performed a new co-variate using linear models. As reported in the Fig. S6, this analysis revealed that, independently by age, the LPC, LPC-O and PC-O panel reduction remain significantly associated with the outcome in males in the severe non-survivor group. This result is in agreement with previous observations [23]. Moreover, the top features for the ML model remain unchanged regardless of patient demographic and reflected the severity and outcome trend (Fig. S7).

3.5. Comparison with results from other Covid-19 patient cohorts

COVID-19 evolves rapidly and dramatically, so the identification of early markers capable of predicting the patient's trajectory is essential. The target of our study was to identify a potential lipidomic signature that could mirror the severity and predict the short-term mortality of COVID-19 disease at the time of hospitalization, by using untargeted lipidomics, through the employment of a RP-UHPLC-TIMS-MS approach which adds further confidence to lipid annotation [24]. We found that, among the different lipid classes, glycerophospholipids were the most discriminant between mild and severe conditions as well as with respect to non-COVID-19 patients; in particular several LPCs, LPC-Os and PC-O were the lipids with highest statistical significance, with a progressive decrease in relation to the severity status. Then, we sought if the lipidome signature could be used as a prognostic tool to identify potential progression from mild to severe condition and intra-hospital mortality. Using the entire dataset, we built a machine learning model that showed reasonable accuracy to predict the disease state. Interestingly, using a restricted panel of six lipids selected across the entire lipid profile, the model showed the comparable results for severity and outcome. COVID-19 pathogenesis is still not completely understood, and lipids play a key role for SARS-CoV2 replication [25] as observed for other human coronavirus infections [26], suggesting that SARS-CoV2 hijacks the host's lipid metabolism [27, 28]. Indeed, lipidic profile can mirror a patient's biological status where internal and/or external perturbations activate molecular pathways involved in the immune response and metabolism. Our results show changes in LPCs and PCs in COVID-19 patients, and in particular, lower-level predicts intra-hospital mortality. A similar pattern was observed in patients with Ebola Virus Disease (EVD), where liver dysfunction and decay of choline metabolism affect LPCs and PCs synthesis and are associated with the severity of the disease. Furthermore, the following increase in LPCs and PCs in survivors confirm their potential use as a marker of severity [5]. Similarly, changes in LPCs and PCs in our cohort of COVID-19 patients can reflect the biological status and predict severity and mortality. Recently, several studies carried out in Italian cohorts investigated the possible relationship of lipidic profiles and infection-pathology severity revealing the alterations in serum concentrations of different lipids [16, 7]. With respect to these studies, our findings highlight the significant decrease of LPCs, LPC-Os and PC-Os concentration, which could be an essential aspect to monitor during COVID-19 disease progression. Our data fits with the observations found in Canadian and Brazilian cohorts [29, 30], both reporting a depressed plasma LPCs profile between COVID-19 and healthy patients. In addition, Sindelar et al. observed of a V-shape trend of LPCs profile after patient recovery from severe status [21], which fully support the important role of changed lipids profile in our study, across survivors and non-survivors patients. Furthermore, our data underline that within the entire lipidome signature, not only LPCs, but specifically ether linked lipids such as LPC-Os and PC-Os owns the highest accuracy in discriminating both severity and outcome. Previous Targeted-MS based lipidomics studies were conducted to distinguish between asymptomatic COVID-19 and healthy subjects, or in

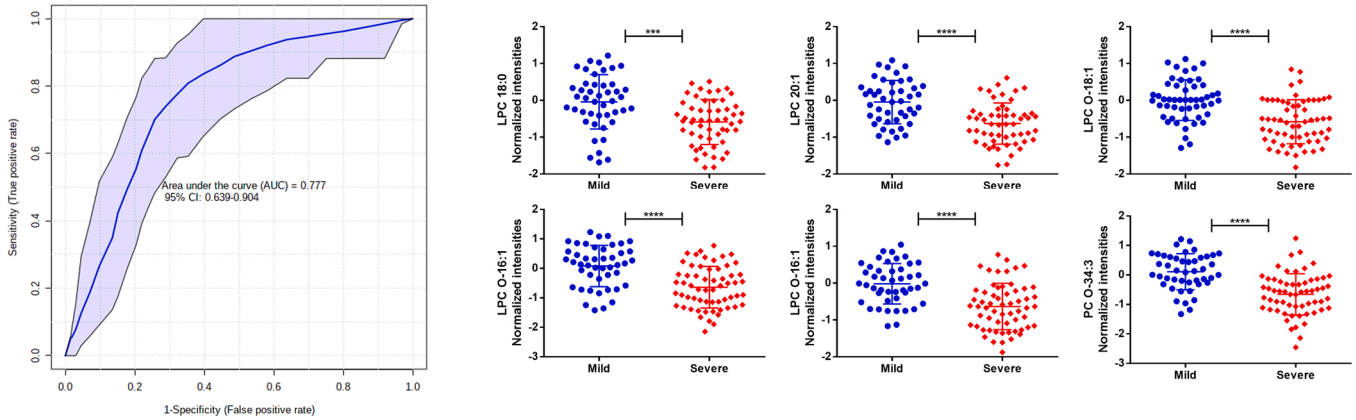

Fig. 5. ROC curves for severity obtained with the predictive model (RF) on the reduced lipid panel composed by LPC O-18:1, PC O-34:3, LPC 20:1, LPC O-16:1, LPC 18:0, LPC O-16:0 and comparison of normalized intensity of the selected lipid panel in survivors compared to non-survivor patients in Mild (blue) and Severe (red) patients (***$p < 0.001$; ****: $p < 0.0001$).

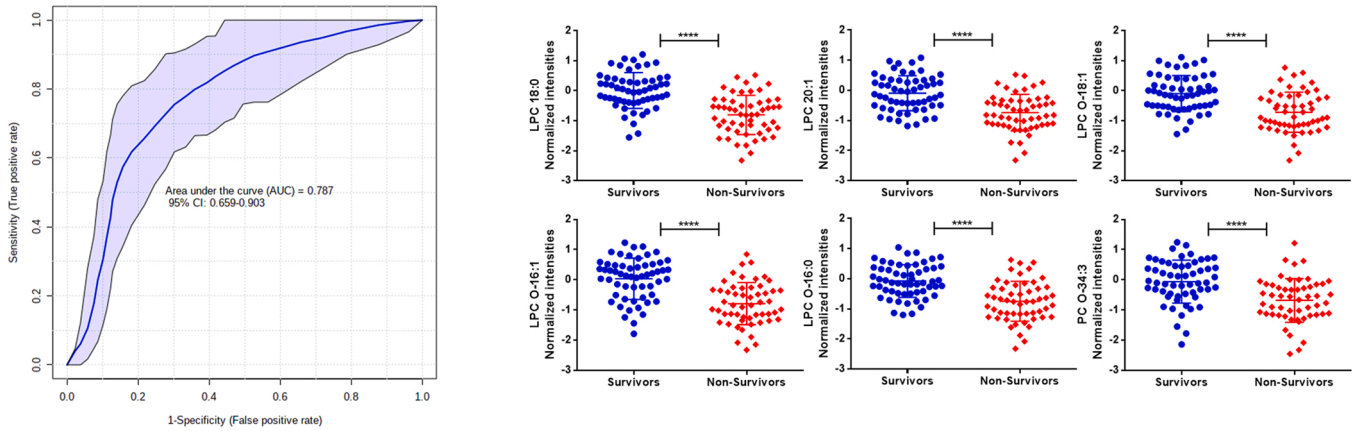

Fig. 6. ROC curves for outcome obtained with the predictive model (RF) on the reduced lipid panel composed by LPC O-18:1, PC O-34–3, LPC 20:1, LPC O-16–1, LPC 18:0, LPC O-16:0 and comparison of normalized intensity of the selected lipid panel in survivors compared to non-survivor patients in Survivors (blue) and Non-Survivors (red) patients (****: $p < 0.0001$).

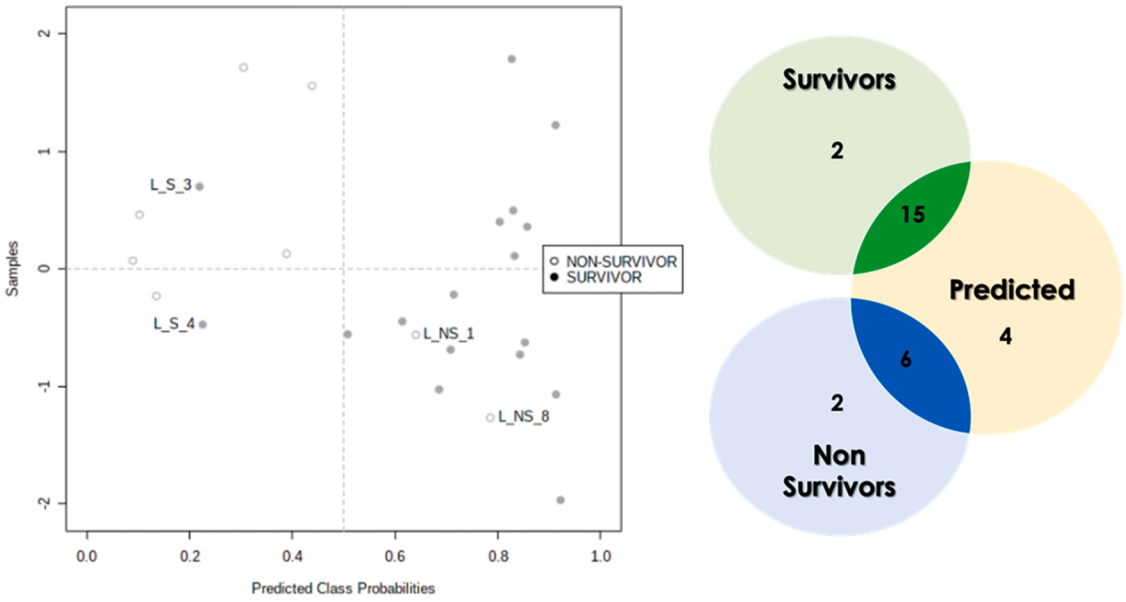

Fig. 7. Confusion matrix representing the performance of the model applied to 25 longitudinal (t1) COVID-19 patients. Samples classified into the wrong group were labeled (S: survivor, NS: non-survivor).

diagnostics, to discriminate symptomatic COVID-19 and healthy patients, as a new tool to augment RT-PCR strategy [31]. In other studies, with comparable numbers of patients, different proteomic and metabolomic profiles were demonstrated to be associated with clinical phenotypes of COVID-19, from mild to severe [32]. While previous lipidomics studies reported the observation of relative fold-changes of detected lipids between different study groups, the comparison of lipid concentration, is essential to support inter study comparison [19–33]. Nevertheless, only few studies have reported concentration data (as nmol/mL), and hence comparison is not possible. In this regard our data partially agree with results of Barberis et al. [16], but differences have been observed with available data to the use of different I.S, hence our data could be useful for comparison with future observations or follow-up. Our study, while of relatively small size but comparable to other studies, is the first to propose, to our knowledge, that a restricted subset of six lipids (LPC O-18:1, PC O-34:3, LPC 20:1, LPC O-16:1, LPC 18:0, LPC O-16:0) not highlighted previously, could potentially predict intra-hospital mortality already at the time of the admission, in both mild and severe COVID-19 patients, and identify those patients requiring tight monitoring and/or intensive treatment. Clearly, our results are based on a single Italian cohort of COVID-19 patients, thus future studies with larger cohorts including different racial, ethnic, and geographical cohorts will be necessary for extending our current understanding of lipid metabolic dysregulation. In addition, the number of healthy subjects is relatively small, but comparable in age difference with previous studies which employed as reference group healthy COVID(-) patients [16–21]. Before the translation to clinical settings, the prognostic value of the identified lipid panel on COVID-19 outcome should be applied to large and separate patients' cohorts,

4. Conclusions

In this work an untargeted lipidomics analysis by RP-UHPLC-TIMS-MS was performed on a cohort of COVID-19 patients with different severity. Our results unveiled a panel of LPCs, LPC-Os and PC-O predicting the severity and mortality in hospitalized COVID-19 patients. This simplified lipid panel could find potential employment as a predictive tool in faster, targeted approaches, such as using multiple reaction monitoring (MRM) strategies, to obtain absolute quantitative data that could be easier employed in a clinical setting. While our approach

can be defined untargeted, allowing identification and quantification of different lipid classes, particular lipid sub-classes could be not detected such as oxylipins, that require targeted or pseudo targeted approaches, and other were excluded due to absence of adequate internal standards. In addition, other important polar metabolites could be included in the analysis, such as amino acids and acylcarnitines, to enrich the model.

Funding

This work was funded by The Italian Ministry of Education, Universities and Research (MIUR) project: PIR01_00032 - BIO OPEN LAB - BOL "CUP" J37E19000050007 to P. Campiglia.

CRediT authorship contribution statement

Conceptualization: P.C, C.V, M.C, A.C and E.SO. Formal analysis: M. C, C.I, C.V, G.S, D.B, B.P, S.P, P.P, S.M, V.S, G.S and O.P. Investigation: P. D.P, R.M, A.T, E.V and P.I. Data curation: V.C, A.R, F.M, P.D.P, A.T. Supervision: M.C, A.C. Writing - review & editing: A.C, M.C, E.SA, E.SO, PDP. Funding acquisition: P.C, C.V.

Acknowledgments

None.

Conflict of Interest

The authors declare that they have no known competing financial interests or personal relationships that could have appeared to influence the work reported in this paper.

Appendix A. Supporting information

Supplementary data associated with this article can be found in the online version at doi:10.1016/j.jpba.2022.114827.

References

[1] E. Livingston, K. Bucher, Coronavirus disease 2019 (COVID-19) in Italy, JAMA 323 (2020) 1335, https://doi.org/10.1001/jama.2020.4344.
[2] J.S. Ayres, A metabolic handbook for the COVID-19 pandemic, Nat. Metab. 2 (2020) 572–585, https://doi.org/10.1038/s42255-020-0237-2.
[3] S. Lodge, P. Nitschke, T. Kimhofer, J.D. Coudert, S. Begum, S. Bong, T. Richards, D. Edgar, E. Raby, M. Spraul, H. Schaefer, J.C. Lindon, R.L. Loo, E. Holmes, J. K. Nicholson, NMR spectroscopic windows on the systemic effects of SARS-CoV-2 infection on plasma lipoproteins and metabolites in relation to circulating cytokines, J. Proteome Res. 20 (2021) 1382–1396, https://doi.org/10.1021/acs.jproteome.0c00876.
[4] S. De Bruin, L.D. Bos, M.A. Van Roon, A.M. Tuip-De Boer, A.R. Schuurman, M.J. A. Koel-Simmelinck, H.J. Bogaard, P.R. Tuinman, M.A. Van Agtmael, J. Hamann, C.E. Teunissen, W.J. Wiersinga, A.H. Koos Zwinderman, M.C. Brouwer, D. Van De Beek, A.P.J. Vlaar, Clinical features and prognostic factors in COVID-19: a prospective cohort study, EBioMedicine 67 (2021), 103378, https://doi.org/10.1016/j.ebiom.2021.103378.
[5] J.E. Kyle, K.E. Burnum-Johnson, J.P. Wendler, A.J. Eisfeld, P.J. Halfmann, T. Watanabe, F. Sahr, R.D. Smith, Y. Kawaoka, K.M. Waters, T.O. Metz, Plasma lipidome reveals critical illness and recovery from human Ebola virus disease, Proc. Natl. Acad. Sci. USA 116 (2019) 3919–3928, https://doi.org/10.1073/pnas.1815356116.
[6] D. Wu, T. Shu, X. Yang, J.X. Song, M. Zhang, C. Yao, W. Liu, M. Huang, Y. Yu, Q. Yang, T. Zhu, J. Xu, J. Mu, Y. Wang, H. Wang, T. Tang, Y. Ren, Y. Wu, S.H. Lin, Y. Qiu, D.Y. Zhang, Y. Shang, X. Zhou, Plasma metabolomic and lipidomic alterations associated with COVID-19, Natl. Sci. Rev. 7 (2020) 1157–1168, https://doi.org/10.1093/nsr/nwaa086.
[7] M. Caterino, M. Gelzo, S. Sol, R. Fedele, A. Annunziata, C. Calabrese, G. Fiorentino, M. D'abbraccio, C. Dell'isola, F.M. Fusco, R. Parrella, G. Fabbrocini, I. Gentile, I. Andolfo, M. Capasso, M. Costanzo, A. Daniele, E. Marchese, R. Polito, R. Russo, C. Missero, M. Ruoppolo, G. Castaldo, Dysregulation of lipid metabolism and pathological inflammation in patients with COVID-19, Sci. Rep. 11 (2021) 2941, https://doi.org/10.1038/s41598-021-82426-7.
[8] A.J. Eisfeld, P.J. Halfmann, J.P. Wendler, J.E. Kyle, K.E. Burnum-Johnson, Z. Peralta, T. Maemura, K.B. Walters, T. Watanabe, S. Fukuyama, M. Yamashita, J. M. Jacobs, Y.M. Kim, C.P. Casey, K.G. Stratton, B.M. Webb-Robertson, M. A. Gritsenko, M.E. Monroe, K.K. Weitz, A.K. Shukla, M. Tian, G. Neumann, J. L. Reed, H. Van Bakel, T.O. Metz, R.D. Smith, K.M. Waters, A. N'jai, F. Sahr, Y. Kawaoka, Multi-platform 'omics analysis of human ebola virus disease pathogenesis, Cell. Host. Microbe 22 (2017), https://doi.org/10.1016/j.chom.2017.10.011 (817-829 e818).
[9] A. Queiroz, I.F.D. Pinto, M. Lima, M. Giovanetti, J.G. De Jesus, J. Xavier, F. K. Barreto, G.B. Canuto, H.R. Do Amaral, A.M.B. De Filippis, D.L. Mascarenhas, M. B. Falcao, N.P. Santos, V.A.C. Azevedo, M.Y. Yoshinaga, S. Miyamoto, L.C. J. Alcantara, Lipidomic analysis reveals serum alteration of plasmalogens in patients infected with ZIKA virus, Front. Microbiol. 10 (2019) 753, https://doi.org/10.3389/fmicb.2019.00753.
[10] A. Rezaei, S. Neshat, K. Heshmat-Ghahdarijani, Alterations of lipid profile in COVID-19: a narrative review, Curr. Probl. Cardiol. 47 (2021) 1–13, https://doi.org/10.1016/j.cpcardiol.2021.100907, 100907.
[11] K.H. Ebrahimi, J.S.O. Mccullagh, A lipidomic view of SARS-CoV-2, Biosci. Rep. 41 (2021), https://doi.org/10.1042/bsr20210953.
[12] Y. Li, Y. Zhang, R. Lu, M. Dai, M. Shen, J. Zhang, Y. Cui, B. Liu, F. Lin, L. Chen, D. Han, Y. Fan, Y. Zeng, W. Li, S. Li, X. Chen, H. Li, P. Pan, Lipid metabolism changes in patients with severe COVID-19, Clin. Chim. Acta 517 (2021) 66–73, https://doi.org/10.1016/j.cca.2021.02.011.
[13] B. Schwarz, L. Sharma, L. Roberts, X. Peng, S. Bermejo, I. Leighton, A. Casanovas-Massana, M. Minasyan, S. Farhadian, A.I. Ko, I.T. Yale, C.S. Dela Cruz, C.M. Bosio, Cutting edge: severe SARS-CoV-2 infection in humans is defined by a shift in the serum lipidome, resulting in dysregulation of eicosanoid immune mediators, J. Immunol. 206 (2021) 329–334, https://doi.org/10.4049/jimmunol.2001025.
[14] M. Holcapek, G. Liebisch, K. Ekroos, Lipidomic analysis, Anal. Chem. 90 (2018) 4249–4257, https://doi.org/10.1021/acs.analchem.7b05395.
[15] J.W. Song, S.M. Lam, X. Fan, W.J. Cao, S.Y. Wang, H. Tian, G.H. Chua, C. Zhang, F. P. Meng, Z. Xu, J.L. Fu, L. Huang, P. Xia, T. Yang, S. Zhang, B. Li, T.J. Jiang, R. Wang, Z. Wang, M. Shi, J.Y. Zhang, F.S. Wang, G. Shui, Omics-driven systems interrogation of metabolic dysregulation in COVID-19 pathogenesis, Cell. Metab. 32 (2020), https://doi.org/10.1016/j.cmet.2020.06.016 (188-202 e185).
[16] E. Barberis, S. Timo, E. Amede, V.V. Vanella, C. Puricelli, G. Cappellano, D. Raineri, M.G. Cittone, E. Rizzi, A.R. Pedrinelli, V. Vassia, F.G. Casciaro, S. Priora, I. Nerici, A. Galbiati, E. Hayden, M. Falasca, R. Vaschetto, P.P. Sainaghi, U. Dianzani, R. Rolla, A. Chiocchetti, G. Baldanzi, E. Marengo, M. Manfredi, Large-scale plasma analysis revealed new mechanisms and molecules associated with the host response to SARS-CoV-2, Int. J. Mol. Sci. 21 (2020), https://doi.org/10.3390/ijms21228623.
[17] V. Matyash, G. Liebisch, T.V. Kurzchalia, A. Shevchenko, D. Schwudke, Lipid extraction by methyl-tert-butyl ether for high-throughput lipidomics, J. Lipid Res. 49 (2008) 1137–1146, https://doi.org/10.1194/jlr.d700041-jlr200.
[18] P.A. Vorkas, G. Isaac, M.A. Anwar, A.H. Davies, E.J. Want, J.K. Nicholson, E. Holmes, Untargeted UPLC-MS profiling pipeline to expand tissue metabolome coverage: application to cardiovascular disease, Anal. Chem. 87 (2015) 4184–4193, https://dx.doi.org/10.1021%2Fac503775m.
[19] M. Cebo, C. Calderón Castro, J. Schlotterbeck, M. Gawaz, M. Chatterjee, M. Lämmerhofer, Untargeted UHPLC-ESI-QTOF-MS/MS analysis with targeted feature extraction at precursor and fragment level for profiling of the platelet lipidome with ex vivo thrombin-activation, J. Pharm. Biomed. Anal. 205 (2021), 114301, https://doi.org/10.1016/j.jpba.2021.114301.
[20] I. Roberts, M. Wright Muelas, J.M. Taylor, A.S. Davison, Y. Xu, J.M. Grixti, N. Gotts, A. Sorokin, R. Goodacre, D.B. Kell, Untargeted metabolomics of COVID-19 patient serum reveals potential prognostic markers of both severity and outcome, Metabolomics 18 (2021) 6, https://doi.org/10.1007/s11306-021-01859-3.
[21] M. Sindelar, E. Stancliffe, M. Schwaiger-Haber, D.S. Anbukumar, K. Adkins-Travis, C.W. Goss, J.A. O'halloran, P.A. Mudd, W.C. Liu, R.A. Albrecht, A. Garcia-Sastre, L. P. Shriver, G.J. Patti, Longitudinal metabolomics of human plasma reveals prognostic markers of COVID-19 disease severity, Cell. Rep. Med. 2 (2021), 100369, https://doi.org/10.1101/2021.02.05.21251173.
[22] G. Iaccarino, G. Grassi, C. Borghi, C. Ferri, M. Salvetti, M. Volpe, Age and multimorbidity predict death among COVID-19 patients: results of the SARS-RAS study of the Italian society of hypertension, Hypertension 76 (2020) 366–372, https://doi.org/10.1161/hypertensionaha.120.15324 (SARS-RAS Investigators.).
[23] C. Gebhard, V. Regitz-Zagrosek, H.K. Neuhauser, R. Morgan, S.L. Klein, Impact of sex and gender on COVID-19 outcomes in Europe, Biol. Sex. Differ. 11 (2020) 29, https://doi.org/10.1186/s13293-020-00304-9.
[24] C.G. Vasilopoulou, K. Sulek, A.D. Brunner, N.S. Meitei, U. Schweiger-Hufnagel, S. W. Meyer, A. Barsch, M. Mann, F. Meier, Trapped ion mobility spectrometry and PASEF enable in-depth lipidomics from minimal sample amounts, Nat. Commun. 11 (2020) 331, https://doi.org/10.1038/s41467-019-14044-x.
[25] M. Abu-Farha, T.A. Thanaraj, M.G. Qaddoumi, A. Hashem, J. Abubaker, F. Al-Mulla, The role of lipid metabolism in COVID-19 virus infection and as a drug target, Int. J. Mol. Sci. 21 (2020) https://dx.doi.org/10.3390%2Fijms21103544.
[26] B. Yan, H. Chu, D. Yang, K.H. Sze, P.M. Lai, S. Yuan, H. Shuai, Y. Wang, R.Y. Kao, J. F. Chan, K.Y. Yuen, Characterization of the lipidomic profile of human coronavirus-infected cells: implications for lipid metabolism remodeling upon coronavirus replication, Viruses 11 (2019), https://doi.org/10.3390/v11010073.
[27] X. Wei, W. Zeng, J. Su, H. Wan, X. Yu, X. Cao, W. Tan, H. Wang, Hypolipidemia is associated with the severity of COVID-19, J. Clin. Lipidol. 14 (2020) 297–304, https://doi.org/10.1016/j.jacl.2020.04.008.
[28] R. Nardacci, F. Colavita, C. Castilletti, D. Lapa, G. Matusali, S. Meschi, F. Del Nonno, D. Colombo, M.R. Capobianchi, A. Zumla, G. Ippolito, M. Piacentini, L. Falasca, Evidences for lipid involvement in SARS-CoV-2 cytopathogenesis, Cell. Death Dis. 12 (2021) 263, https://doi.org/10.1038/s41419-021-03527-9.

[29] D.D. Fraser, M. Slessarev, C.M. Martin, M. Daley, M.A. Patel, M.R. Miller, E. K. Patterson, D.B. O'gorman, S.E. Gill, D.S. Wishart, R. Mandal, G. Cepinskas, Metabolomics profiling of critically Ill coronavirus disease 2019 patients: identification of diagnostic and prognostic biomarkers, Crit. Care Explor. 2 (2020), e0272 https://dx.doi.org/10.1097%2FCCE.0000000000000272.

[30] J. Delafiori, L.C. Navarro, R.F. Siciliano, G.C. de Melo, E.N.B. Busanello, J. C. Nicolau, G.M. Sales, A.N. de Oliveira, F.F.A. Val, D.N. de Oliveira, A. Eguti, L. A. Dos Santos, T.F. Dalçóquio, A.J. Bertolin, R.L. Abreu-Netto, R. Salsoso, D. Baía-da-Silva, F.G. Marcondes-Braga, V.S. Sampaio, C.C. Judice, F.T.M. Costa, N. Durán, M.W. Perroud, E.C. Sabino, M.V.G. Lacerda, L.O. Reis, W.J. Fávaro, W. M. Monteiro, A.R. Rocha, R.R. Catharino, Covid-19 automated diagnosis and risk assessment through metabolomics and machine learning, Anal. Chem. 93 (2021) 2471–2479, https://doi.org/10.1021/acs.analchem.0c04497.

[31] N. Gray, N.G. Lawler, A.X. Zeng, M. Ryan, S.H. Bong, B.A. Boughton, M. Bizkarguenaga, C. Bruzzone, N. Embade, J. Wist, E. Holmes, O. Millet, J. K. Nicholson, L. Whiley, Diagnostic potential of the plasma lipidome in infectious disease: application to acute SARS-CoV-2 infection, Metabolites 11 (2021), https://doi.org/10.3390/metabo11070467.

[32] B. Shen, X. Yi, Y. Sun, X. Bi, J. Du, C. Zhang, S. Quan, F. Zhang, R. Sun, L. Qian, W. Ge, W. Liu, S. Liang, H. Chen, Y. Zhang, J. Li, J. Xu, Z. He, B. Chen, J. Wang, H. Yan, Y. Zheng, D. Wang, J. Zhu, Z. Kong, Z. Kang, X. Liang, X. Ding, G. Ruan, N. Xiang, X. Cai, H. Gao, L. Li, S. Li, Q. Xiao, T. Lu, Y. Zhu, H. Liu, H. Chen, T. Guo, Proteomic and metabolomic characterization of COVID-19 patient sera, Cell 182 (2020), https://doi.org/10.1016/j.cell.2020.05.032 (59-72 e15).

[33] B. Drotleff, J. Illisom, J. Schlotterbeck, R. Lukowski, M. Lämmerhofer, Comprehensive lipidomics of mouse plasma using class-specific surrogate calibrants and SWATH acquisition for large-scale lipid quantification in untargeted analysis, Anal. Chim. Acta 1086 (2019) 90–102, https://doi.org/10.1016/j.aca.2019.08.030.